Electronic Supplementary Information (ESI) for Nanoscale

Electronic Supporting Information

Effect of Rh valence state and doping concentration on the structure and photocatalytic H_2 evolution in (Nb, Rh)-codoped TiO_2 nanorods

Jiquan Huang,*[a,b] Ting Lv,[a] Qiufeng Huang,[a] Zhonghua Deng,[a] Jian Chen,[b] Zhuguang Liu[b] and Wang Guo*[a,b]

a. Fujian Science & Technology Innovation Laboratory for Optoelectronic Information of China, Fuzhou, 350108, P. R. China. E-mail: hjq@fjirsm.ac.cn, guowang@fjirsm.ac.cn

b. Key Laboratory of Optoelectronic Materials Chemistry and Physics, Fujian Institute of Research on the Structure of Matter, Chinese Academy of Sciences, Fuzhou, 350002, P. R. China.

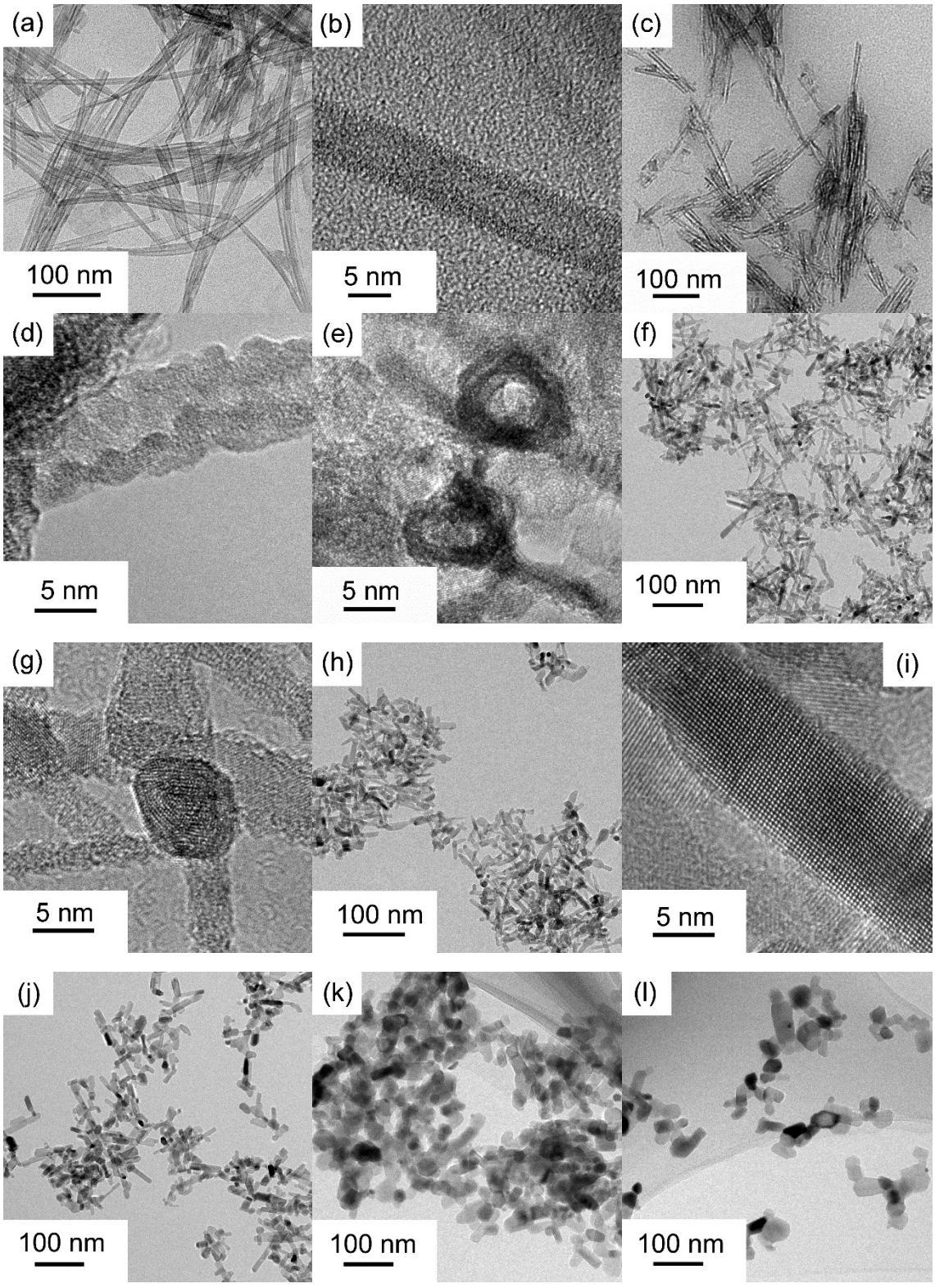

Fig. S1 TEM (a,c,f,h,j,k,l) and HRTEM (b,d,e,g,i) images of protonated titanate nanotubes (a, b) and N6R6TNT ($Ti_{0.988}Nb_{0.006}Rh_{0.006}O_2$) obtained by calcining protonated titanate nanotubes at 400 ^oC (c-e), 500 ^oC (f,g), 600 ^oC (h,i) 700 ^oC (j), 800 ^oC (k), and 900 ^oC (l).

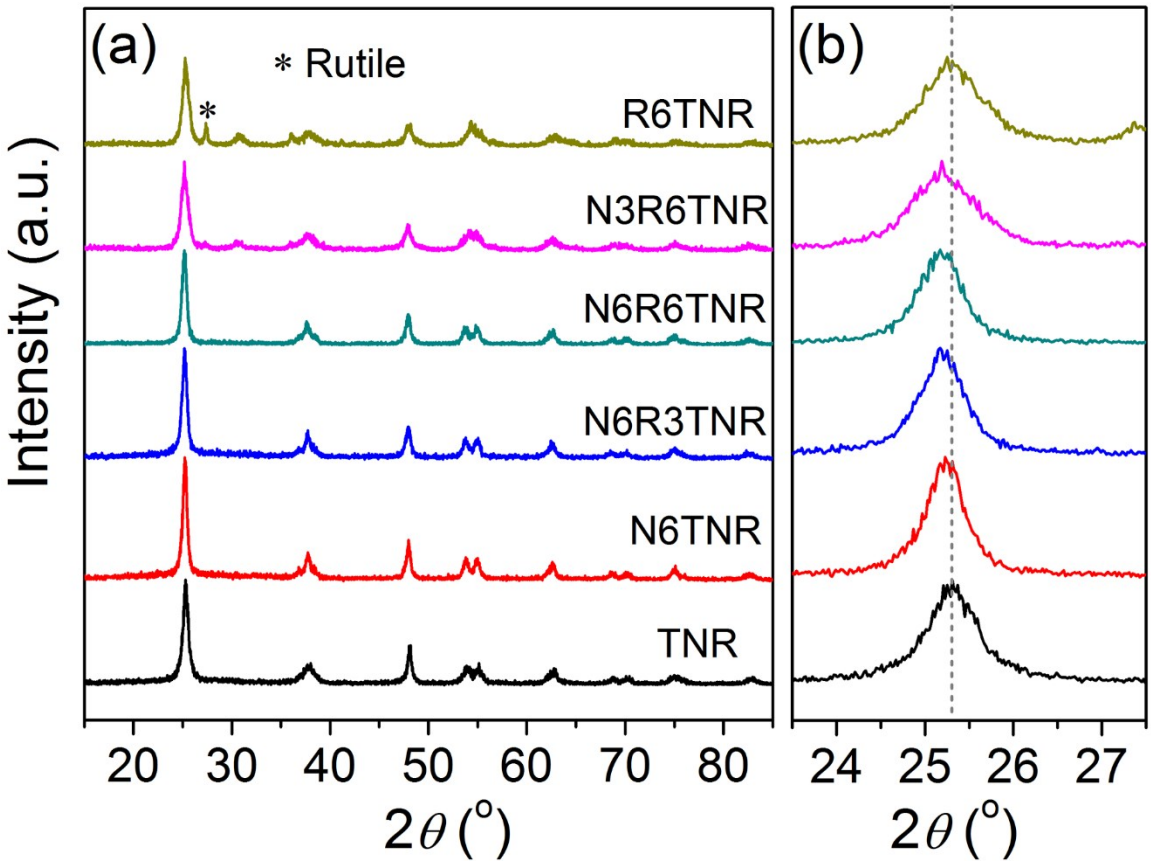

Fig. S2 (a) XRD patterns of TiO_2 and Nb/Rh-doped TiO_2 nanorods with different Nb/Rh ratio. (b) The enlarged patterns around $2\theta = 25.5^{o}$. The samples were calcined at 500 ^{o}C for 2 h.

The effective ionic radius with CN=6 is 0.605 Å for Ti^{4+}, 0.60 Å for Rh^{4+}, 0.665 Å for Rh^{3+}, and 0.64 Å for Nb^{5+}, respectively. The substitution of Nb^{5+} and/or Rh^{3+} for Ti^{4+} will result in the shift of the diffraction peaks to lower angles, while the substitution of Rh^{4+} for Ti^{4+} will not cause an obvious peak shift.

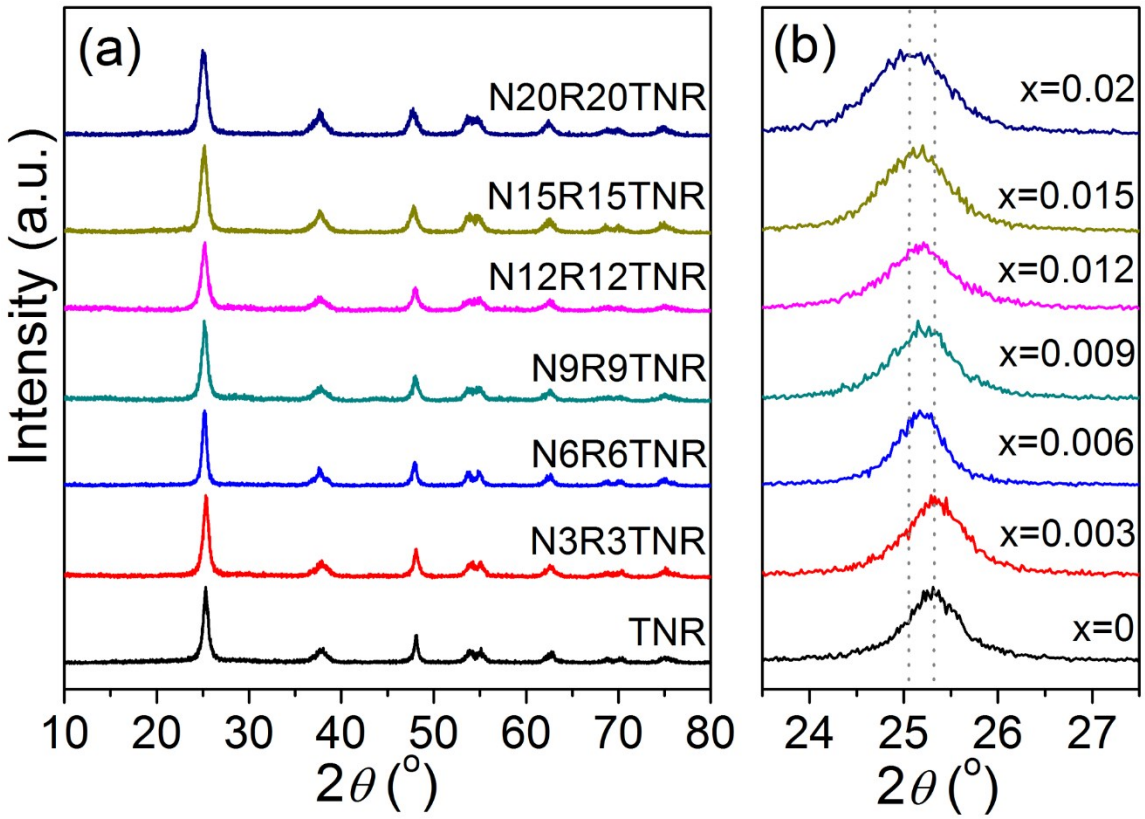

Fig. S3 (a) XRD patterns of Nb/Rh-codoped TiO_2 ($Ti_{1-2x}Nb_xRh_xO_2$) nanorods calcined at 500 °C for 2 h. (b) The enlarged patterns around 2θ = 25.5°.

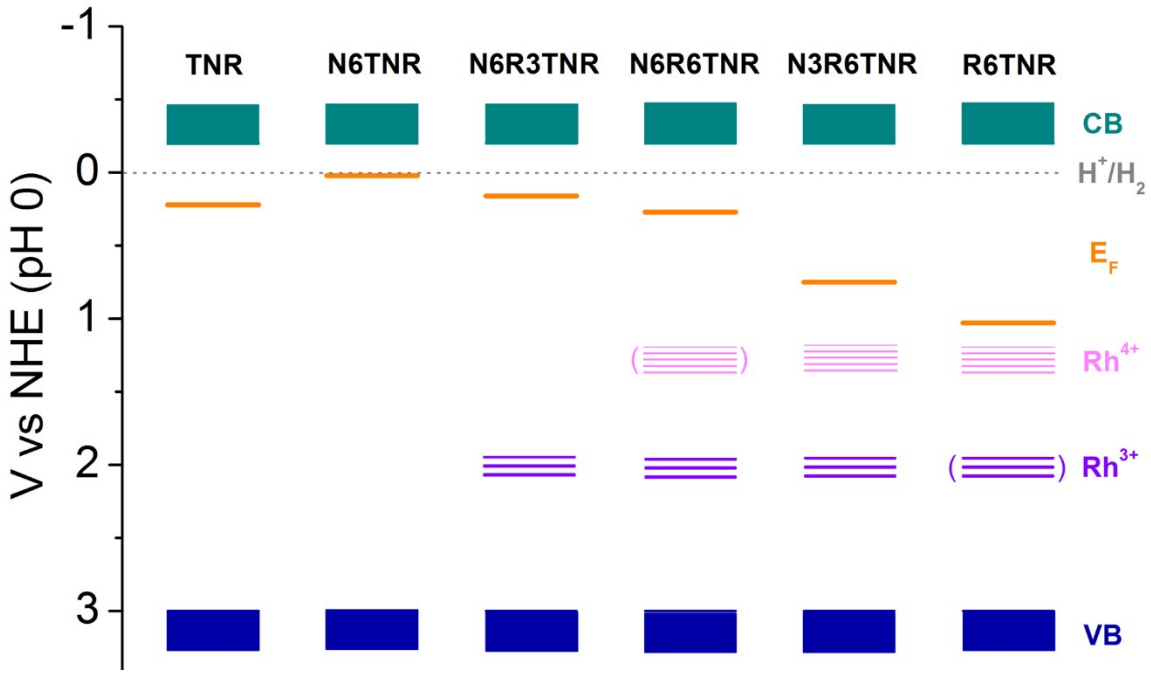

Fig. S4 Proposed band energy diagram of the photocatalysts. The brackets indicate that the low content of the corresponding Rh valence state. In this schematic, the effect of doping on the E_g (band gap) and position of VB (and CB) is neglected.

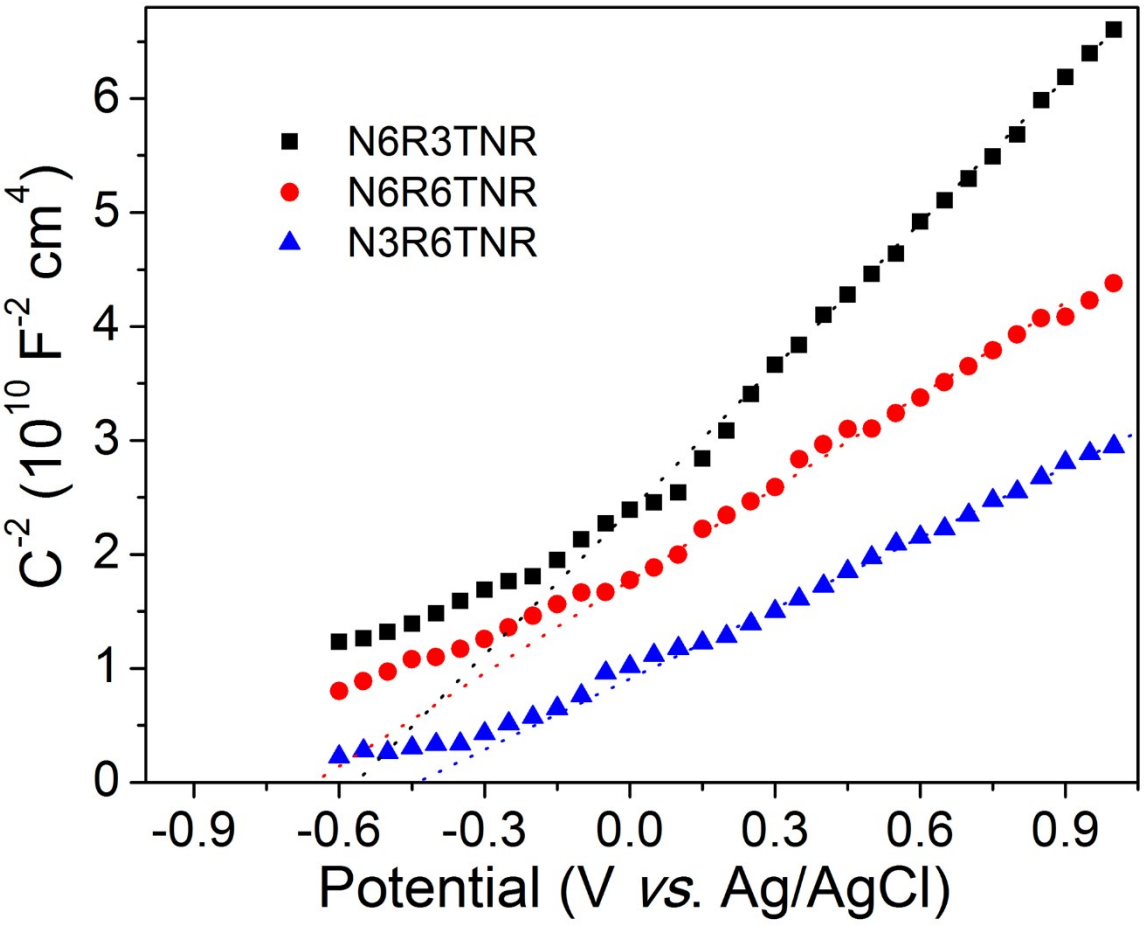

Fig. S5 Mott-Schottky plot for N6R3TNT ($Ti_{0.991}Nb_{0.006}Rh_{0.0033}O_2$), N6R6TNT ($Ti_{0.988}Nb_{0.006}Rh_{0.006}O_2$), and N3R6TNT ($Ti_{0.991}Nb_{0.003}Rh_{0.006}O_2$) at 2000 Hz.

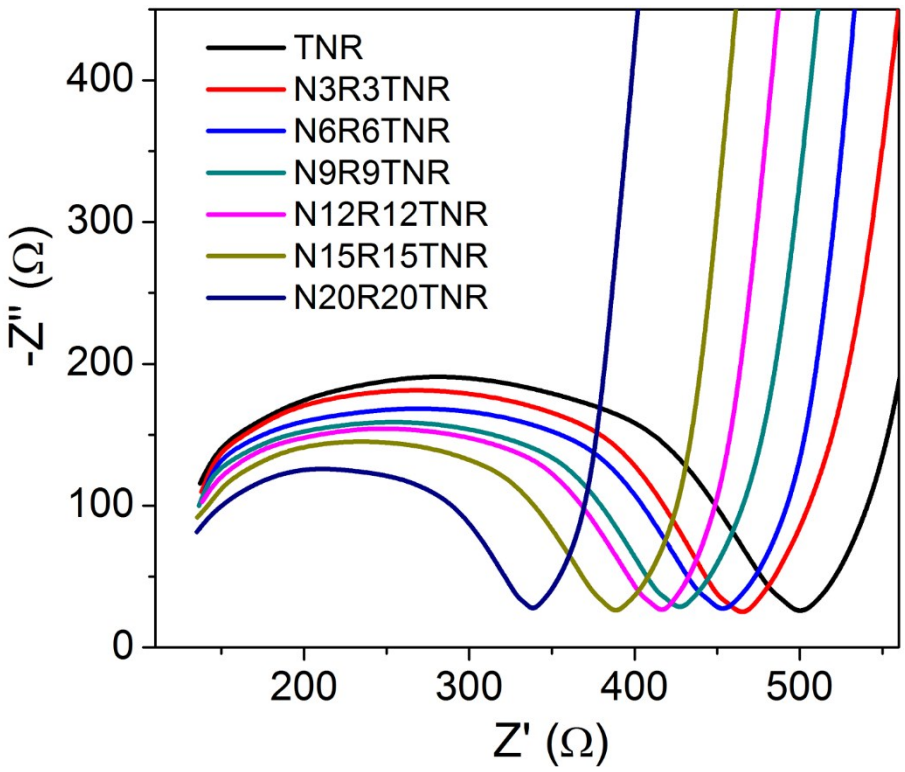

Fig. S6 Nyquist plots for $Ti_{1-2x}Nb_xRh_xO_2$ photocatalysts.

The semicircular diameter of the $Ti_{1-2x}Nb_xRh_xO_2$ photocatalysts decreased with increasing doping concentration (x), which is mainly caused by the increase in Rh(IV) concentration.

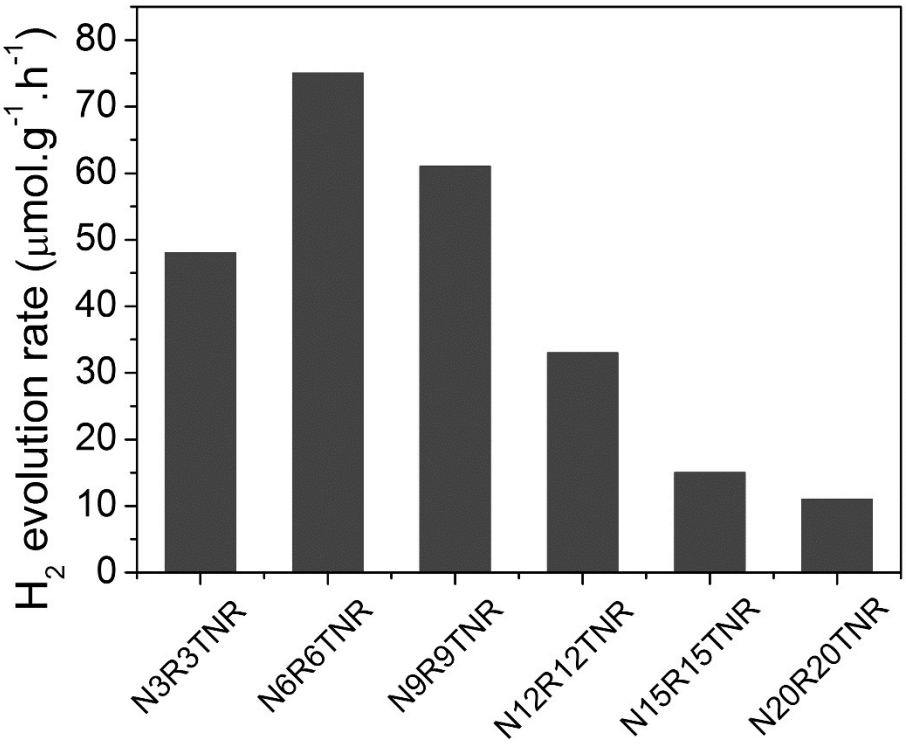

Fig. S7 Visible light driven Hydrogen generation over $Ti_{1-2x}Nb_xRh_xO_2$ photocatalysts from aqueous methanol solution.

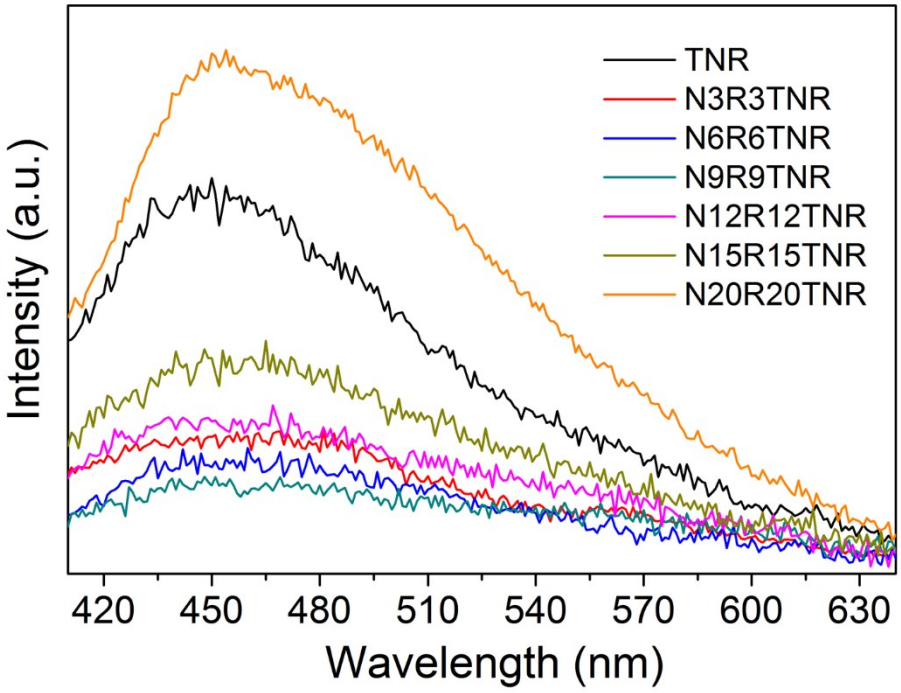

Fig. S8 Photoluminescence spectra of the $Ti_{1-2x}Nb_xRh_xO_2$ photocatalysts under 380 nm excitation.